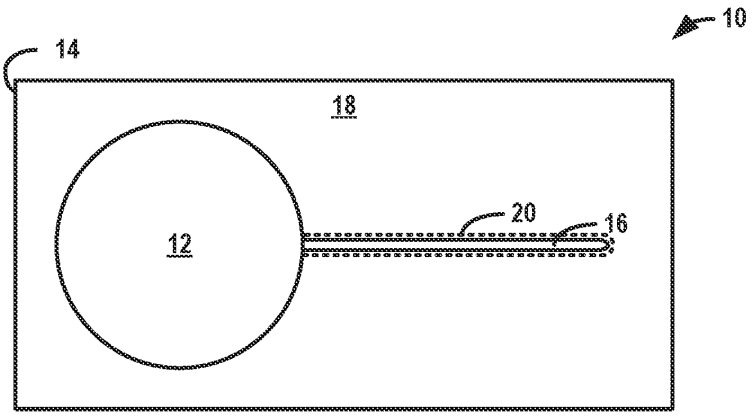

FIG. 1A

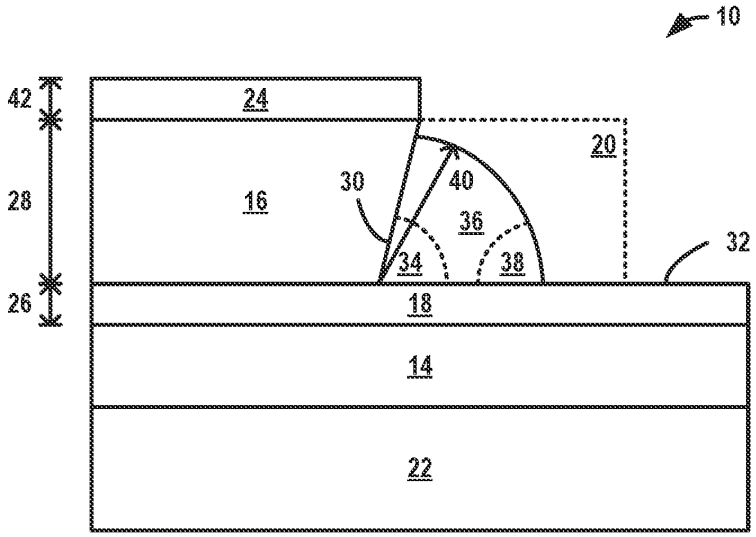

FIG. 1B

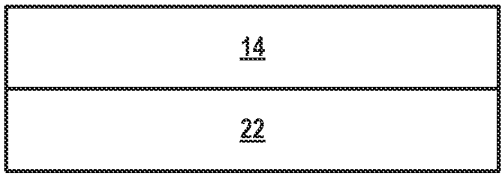

FIG. 2A

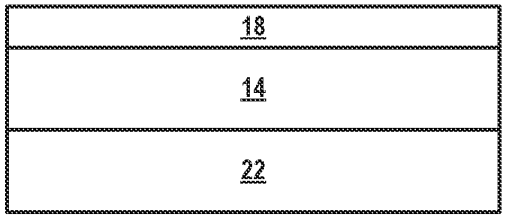

FIG. 2B

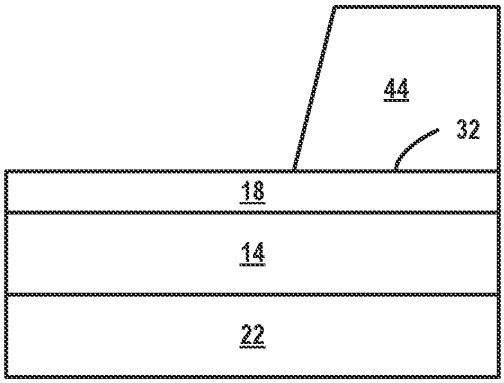

FIG. 2C

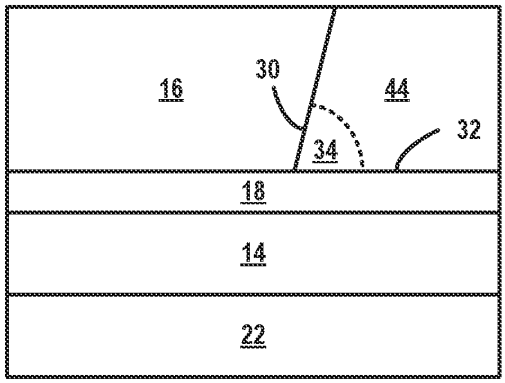

FIG. 2D

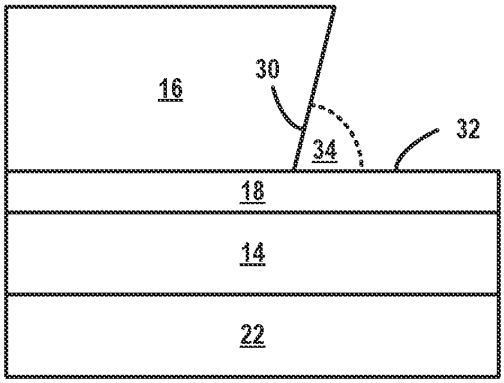

FIG. 2E

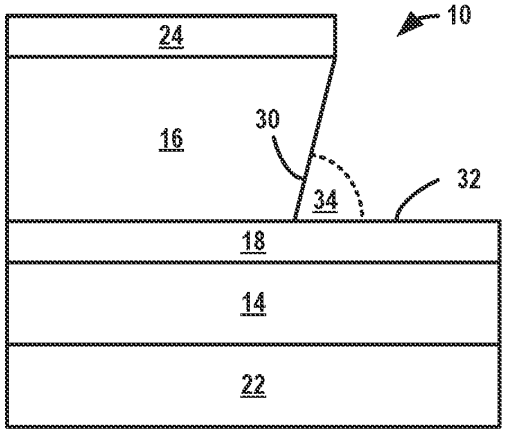

FIG. 2F

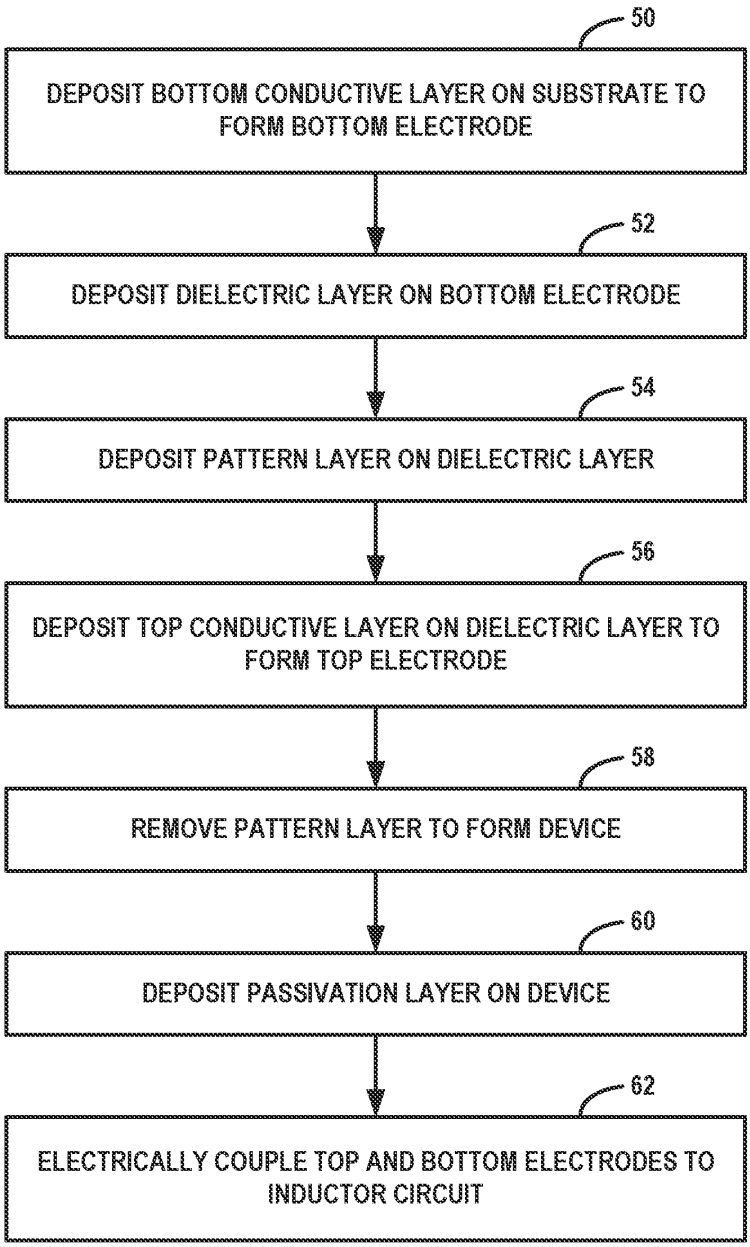
50
DEPOSIT BOTTOM CONDUCTIVE LAYER ON SUBSTRATE TO FORM BOTTOM ELECTRODE
52
DEPOSIT DIELECTRIC LAYER ON BOTTOM ELECTRODE
54
DEPOSIT PATTERN LAYER ON DIELECTRIC LAYER
56
DEPOSIT TOP CONDUCTIVE LAYER ON DIELECTRIC LAYER TO FORM TOP ELECTRODE
58
REMOVE PATTERN LAYER TO FORM DEVICE
60
DEPOSIT PASSIVATION LAYER ON DEVICE
62
ELECTRICALLY COUPLE TOP AND BOTTOM ELECTRODES TO INDUCTOR CIRCUIT

FIG. 3

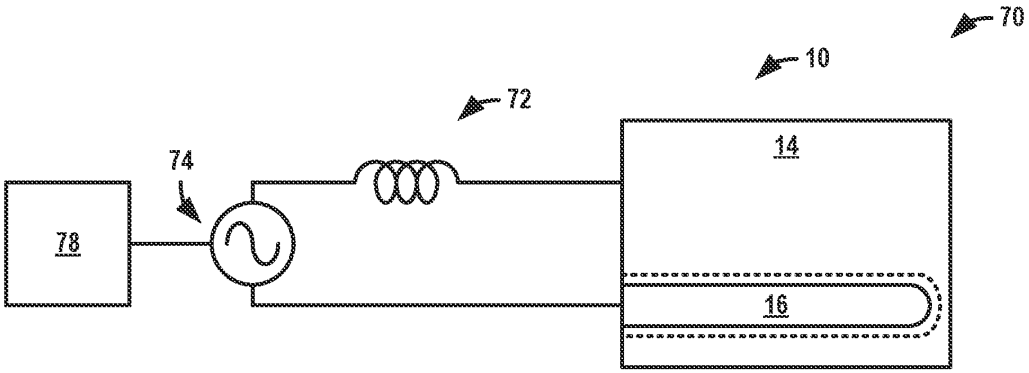

FIG. 4A

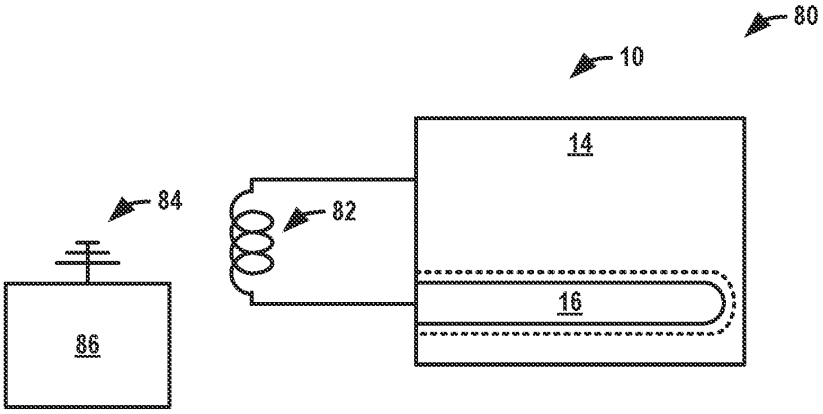

FIG. 4B

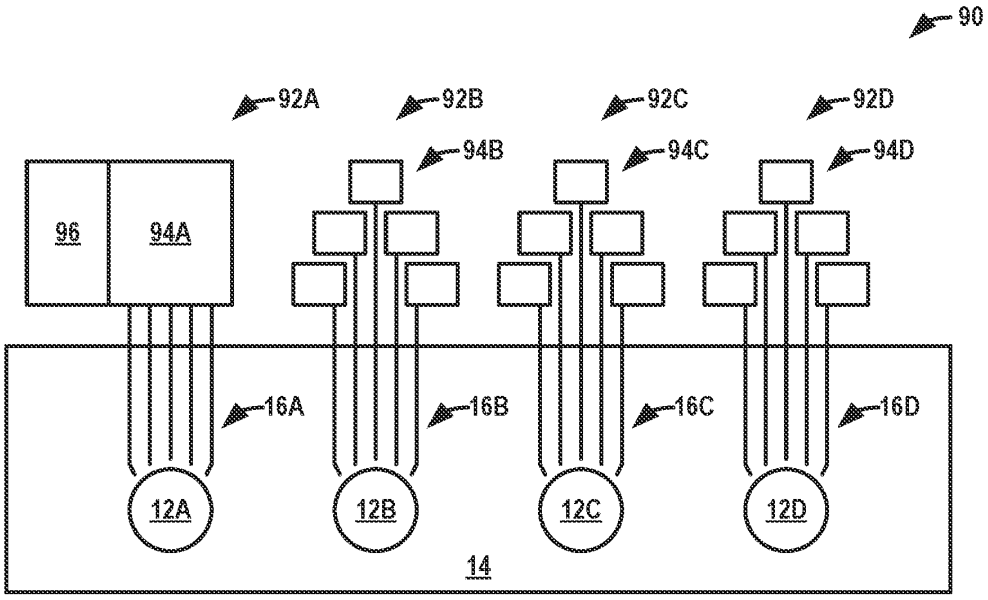

FIG. 5A

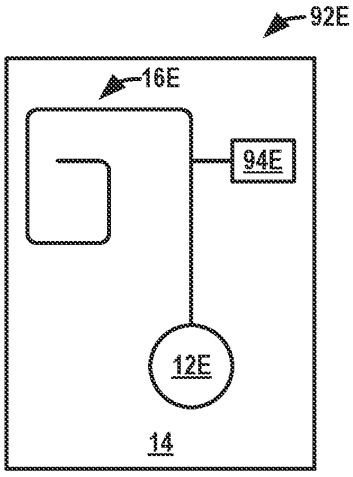

FIG. 5B

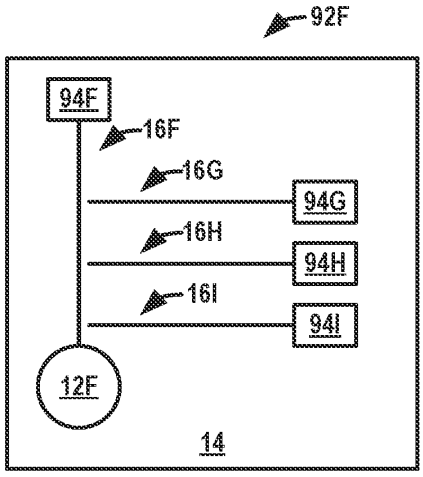

FIG. 5C

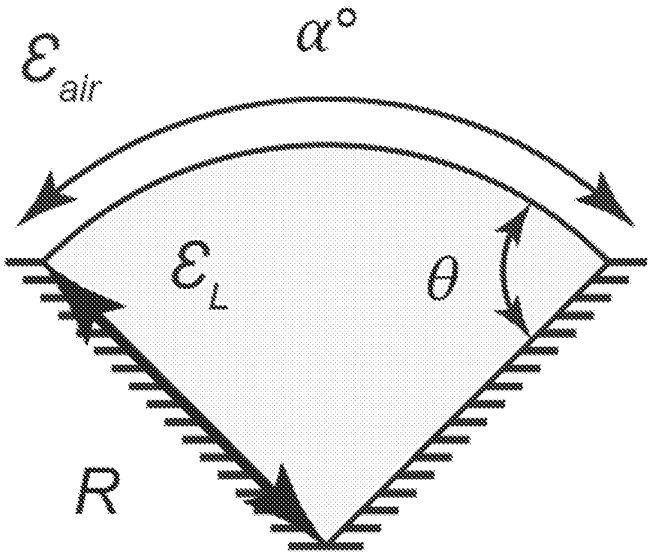
ε_{air}
$\alpha°$
ε_L
θ
R

FIG. 6A

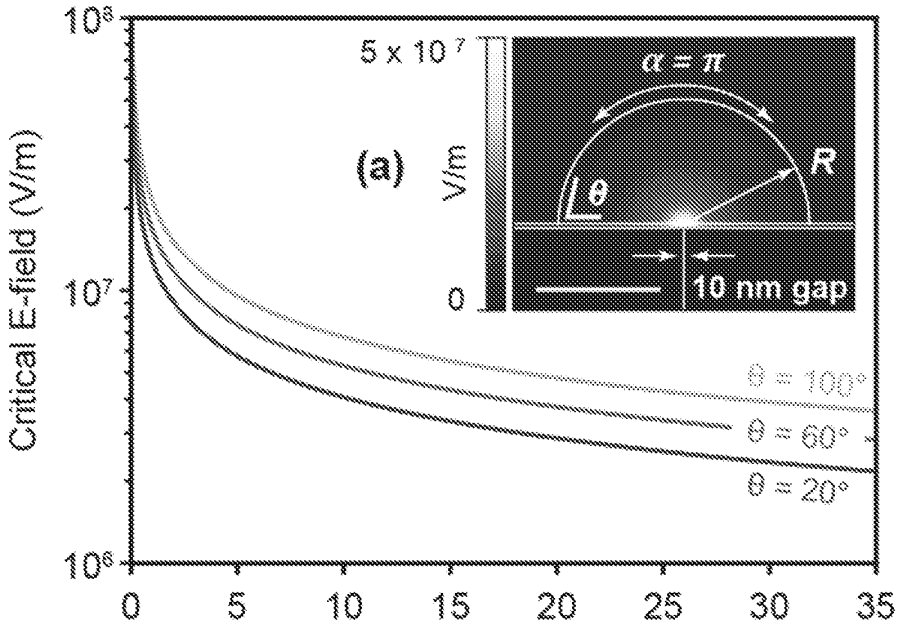
Critical E-field (V/m)
10^8
10^7
10^6
0
5
10
15
20
25
30
35
5 x 10^7
(a)
V/m
0
$\alpha = \pi$
R
θ
10 nm gap
θ = 100°
θ = 60°
θ = 20°

FIG. 6B

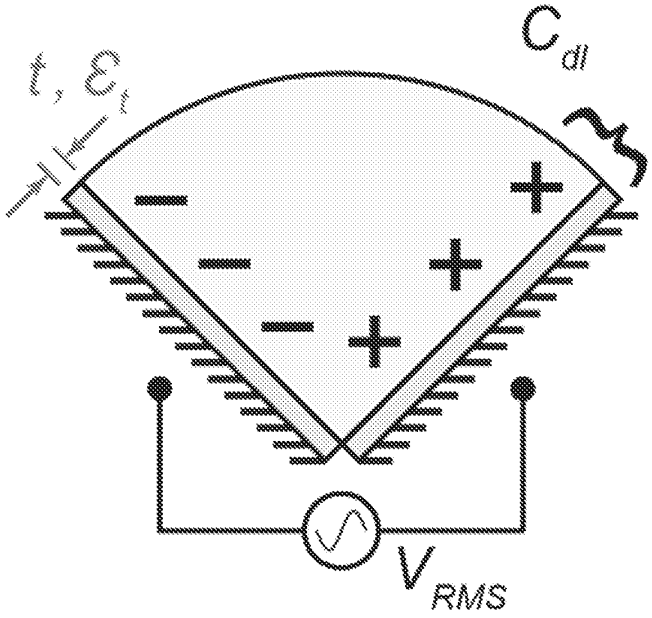
C_{dl}
t, ε_t
V_{RMS}

FIG. 6C

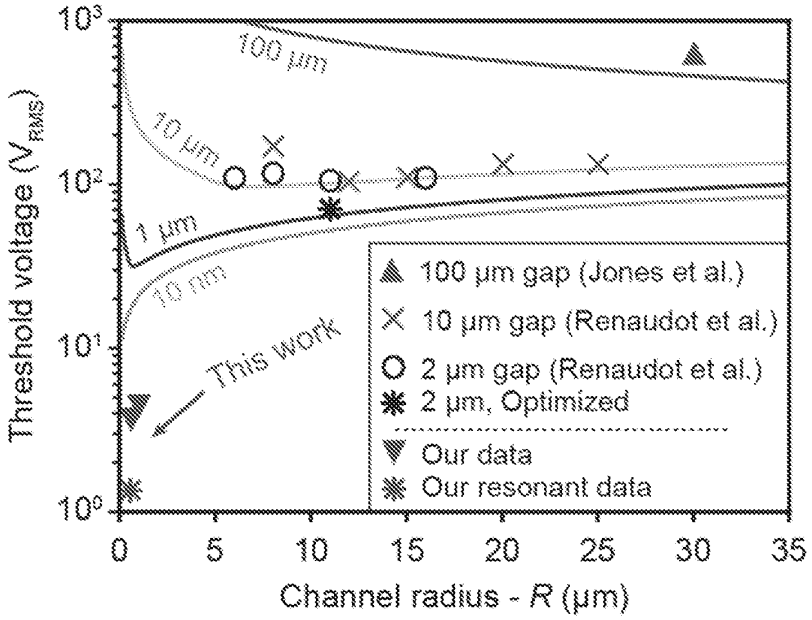
Threshold voltage (V_{RMS})
Channel radius - R (μm)
100 μm
10 μm
1 μm
10 nm
This work
100 μm gap (Jones et al.)
10 μm gap (Renaudot et al.)
2 μm gap (Renaudot et al.)
2 μm, Optimized
Our data
Our resonant data

FIG. 6D

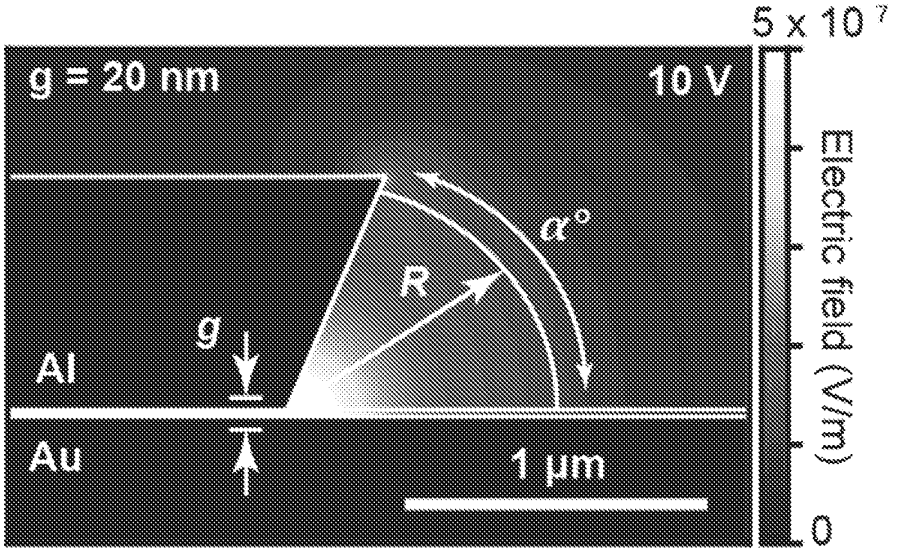
5 x 10 7
g = 20 nm
10 V
α°
R
g
Al
Au
1 μm
Electric field (V/m)
0

FIG. 7A

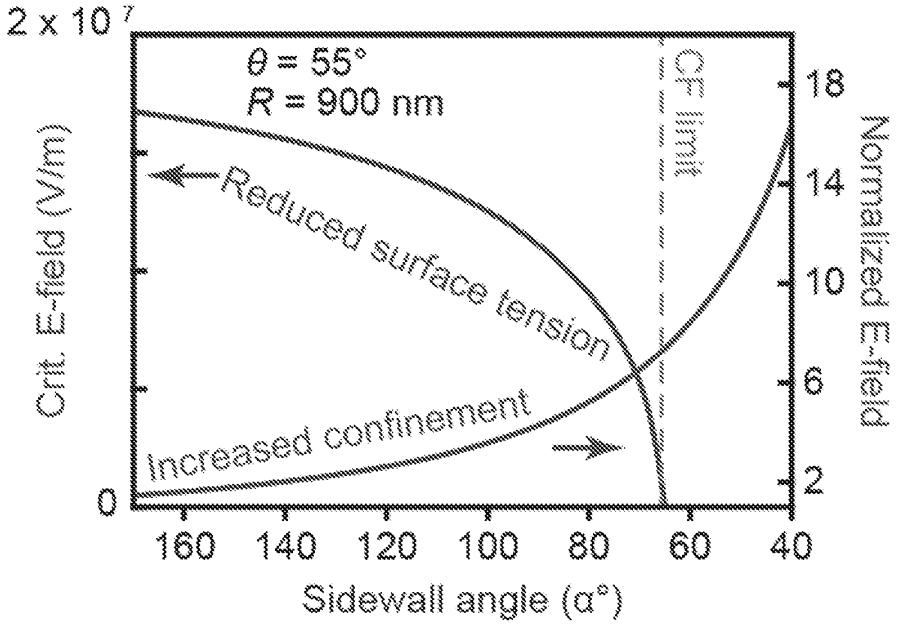
2 x 10 7
θ = 55°
R = 900 nm
CF limit
Reduced surface tension
Increased confinement
Crit. E-field (V/m)
Normalized E-field
0
18
14
10
6
2
160
140
120
100
80
60
40
Sidewall angle (α°)

FIG. 7B

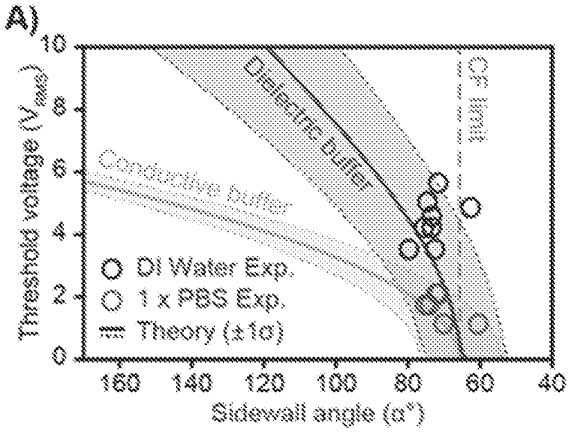

FIG. 8A

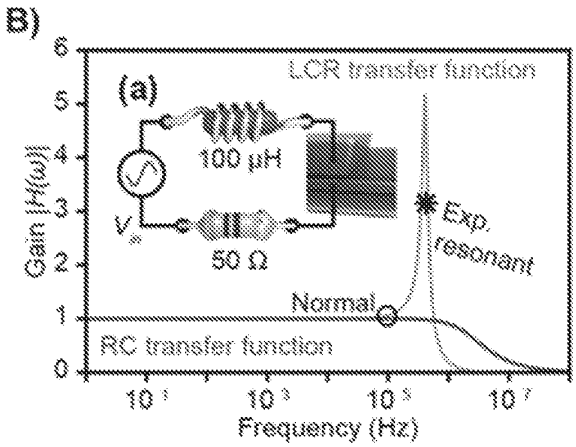

FIG. 8B

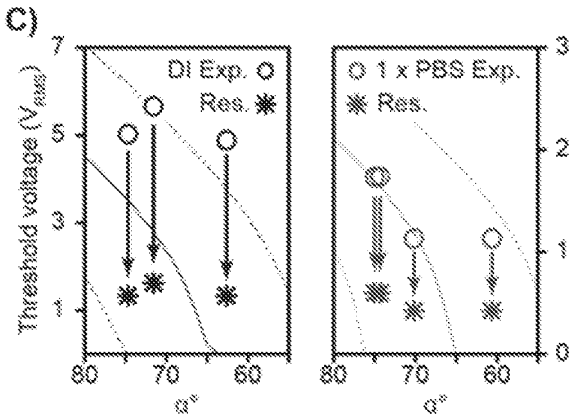

FIG. 8C

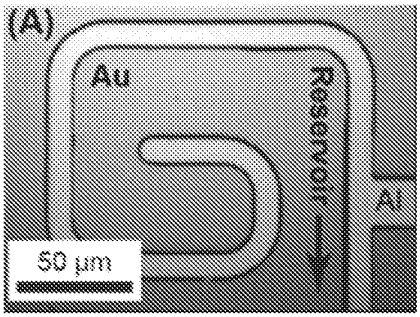

FIG. 9A

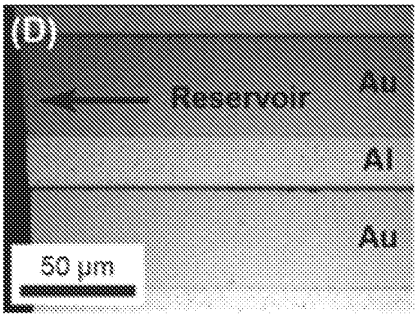

FIG. 9D

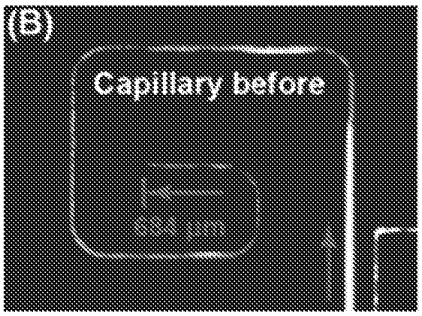

FIG. 9B

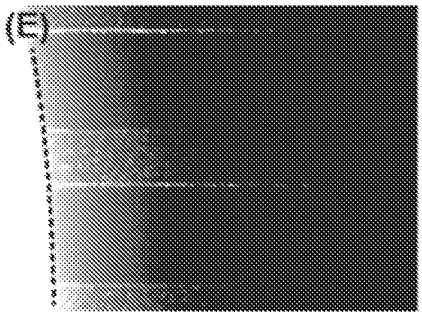

FIG. 9E

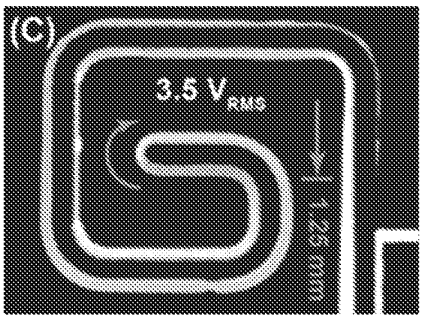

FIG. 9C

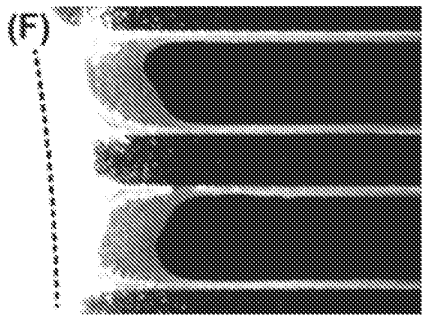

FIG. 9F

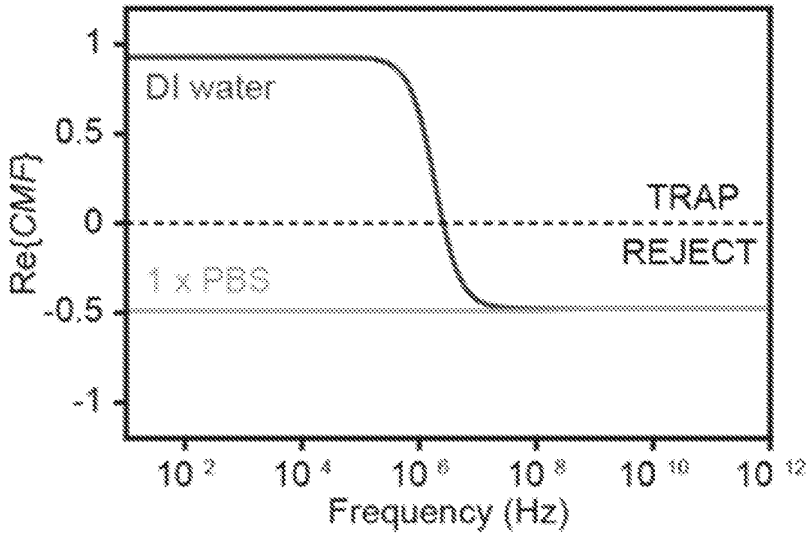

FIG. 10A

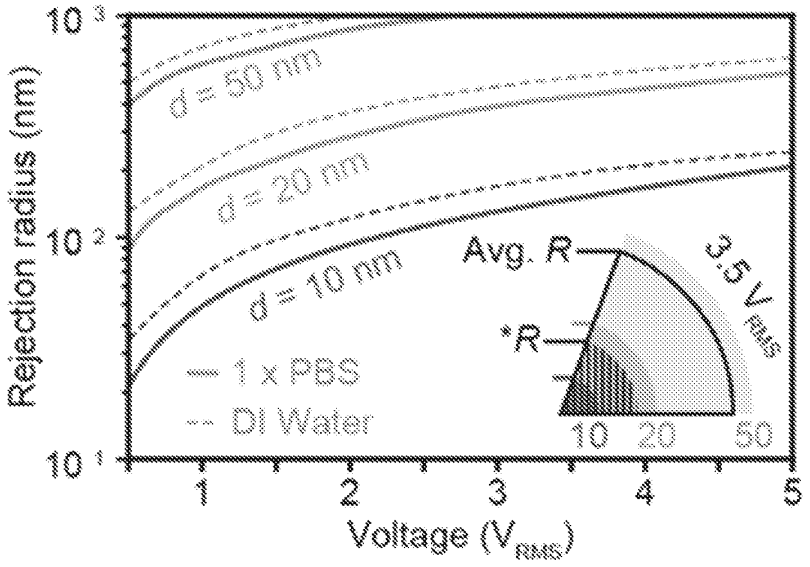

FIG. 10B

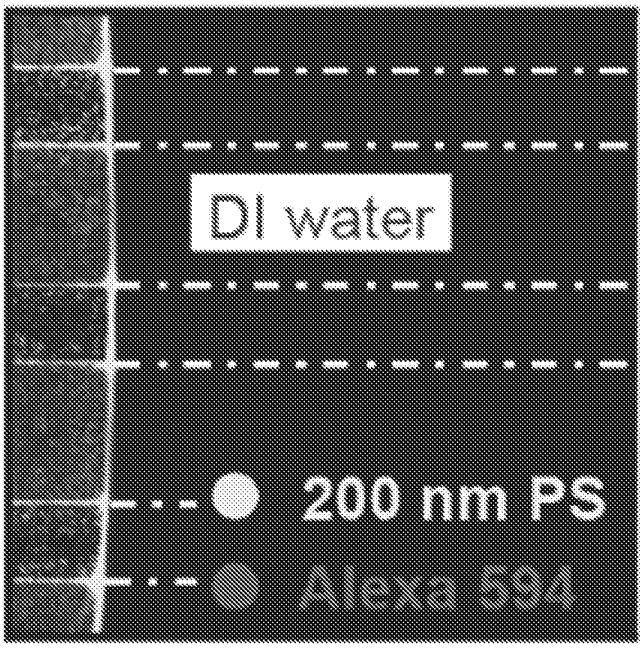

FIG. 10C

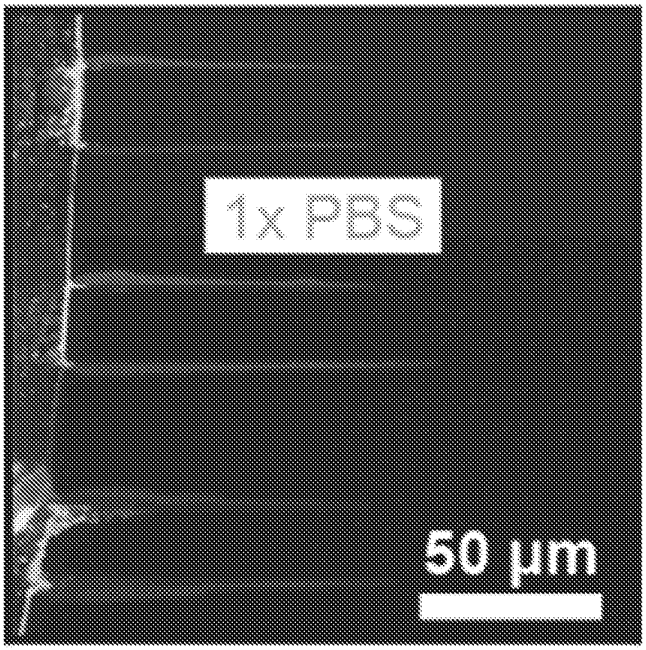

FIG. 10D

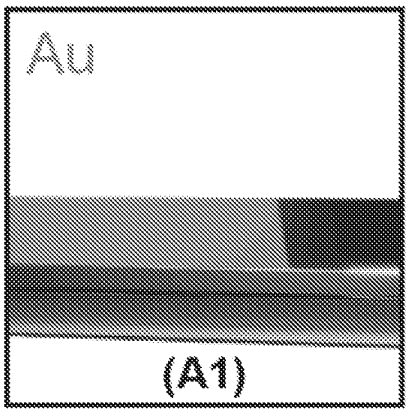

FIG. 11A

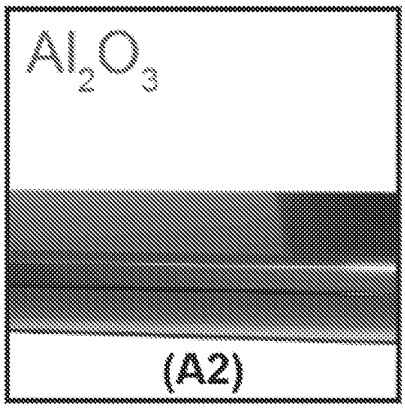

FIG. 11B

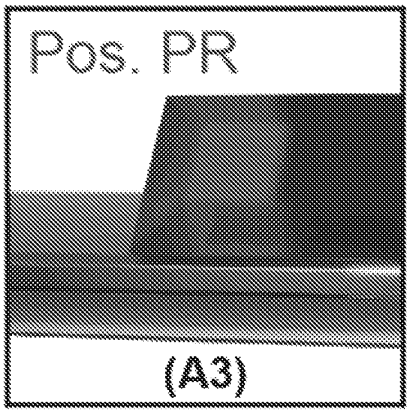

FIG. 11C

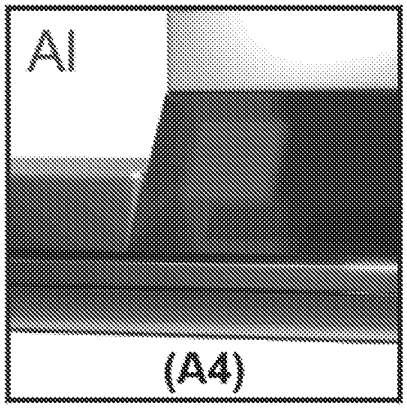

FIG. 11D

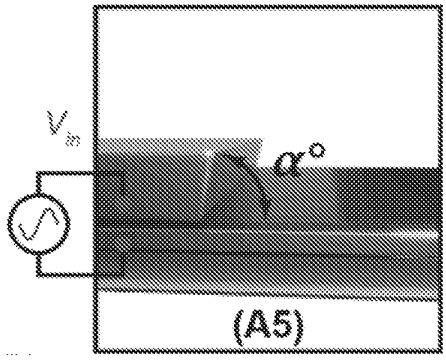

FIG. 11E

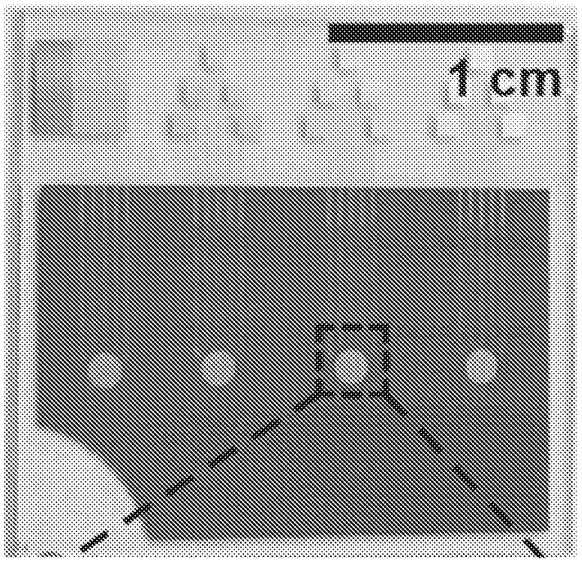

FIG. 12A

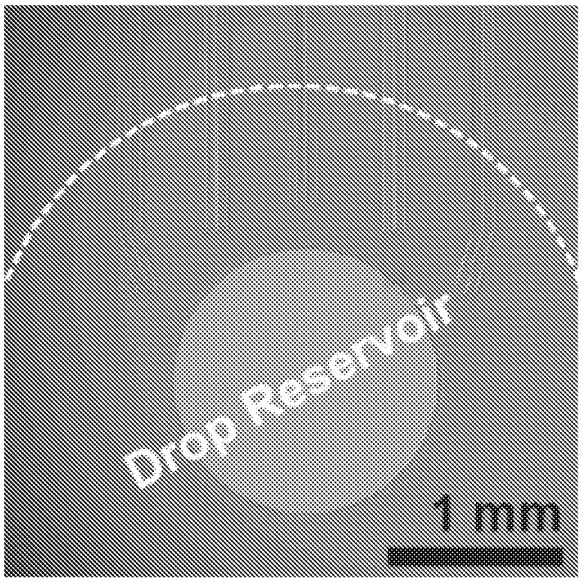

FIG. 12B

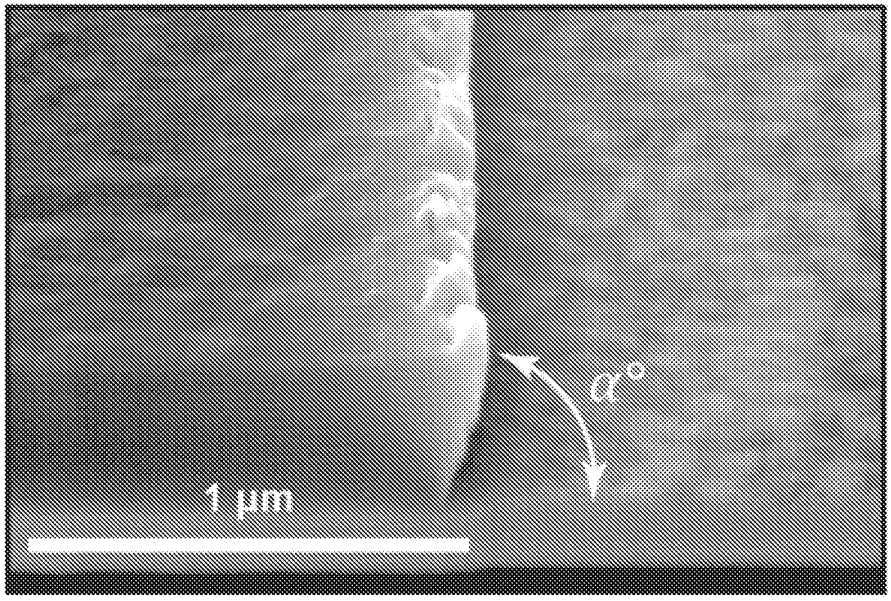

FIG. 12C

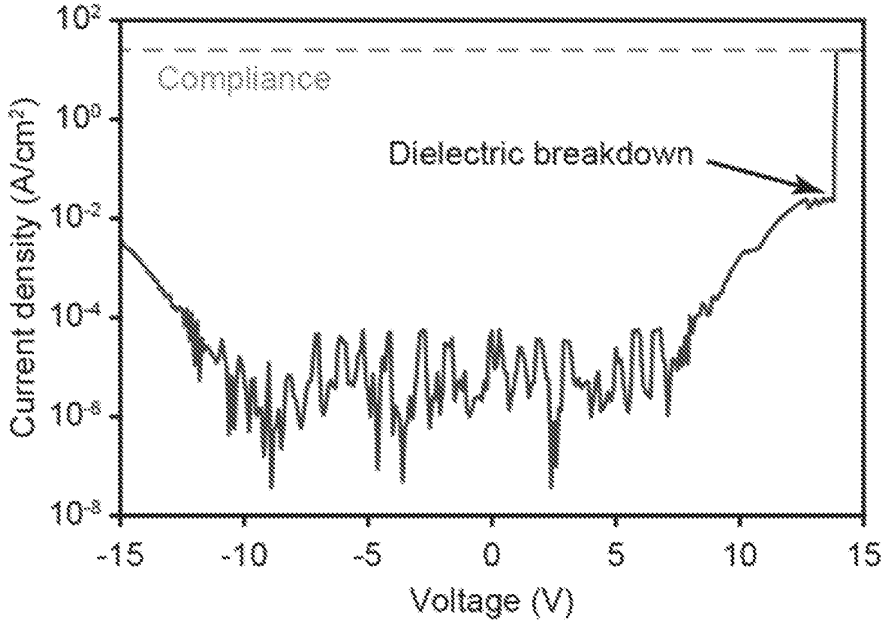

FIG. 12D

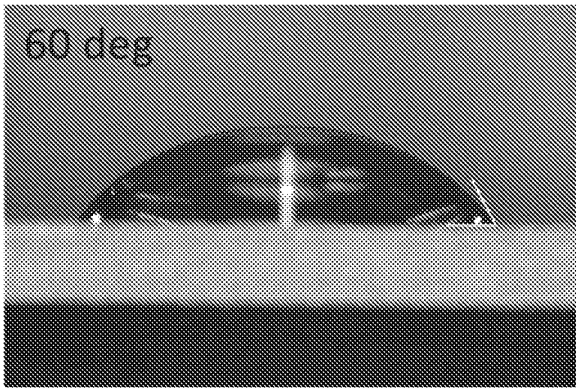

FIG. 13A

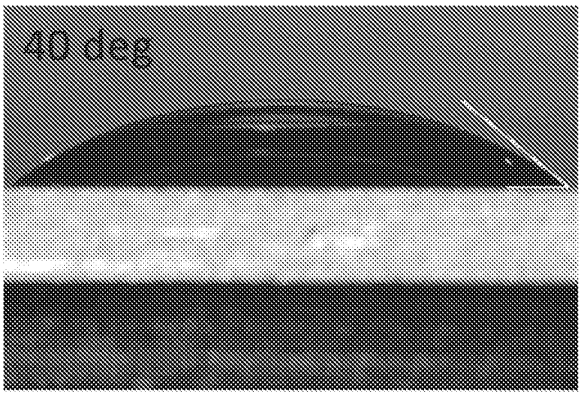

FIG. 13B

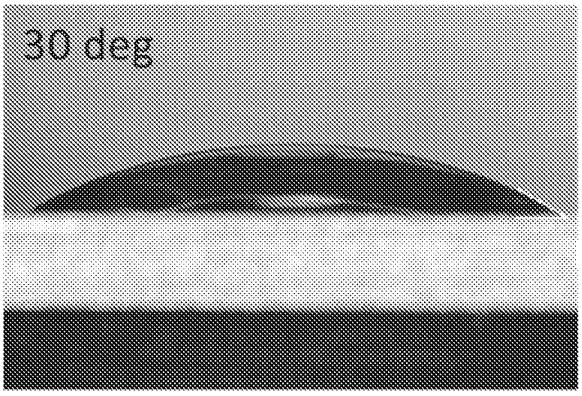

FIG. 13C

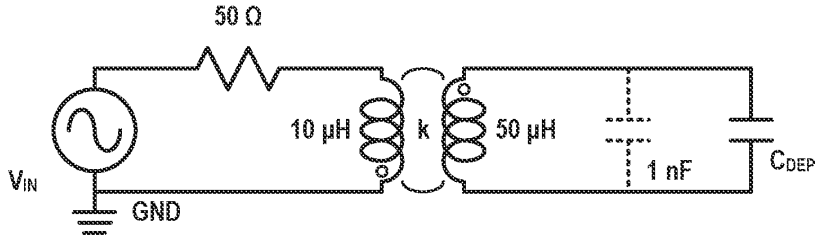

FIG. 14A

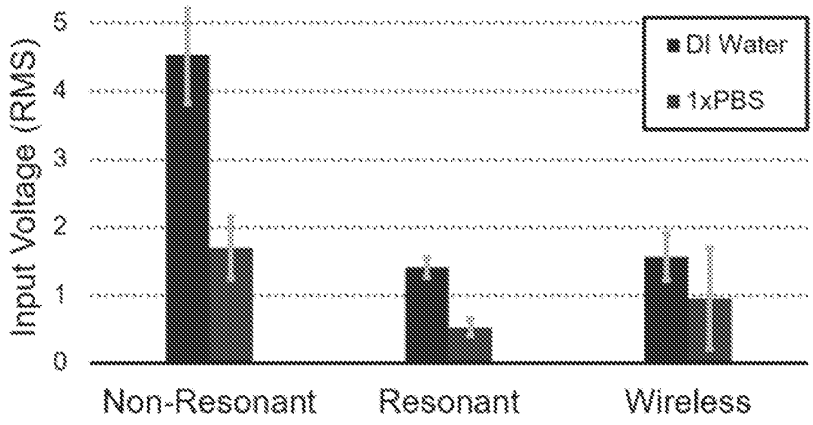

FIG. 14B

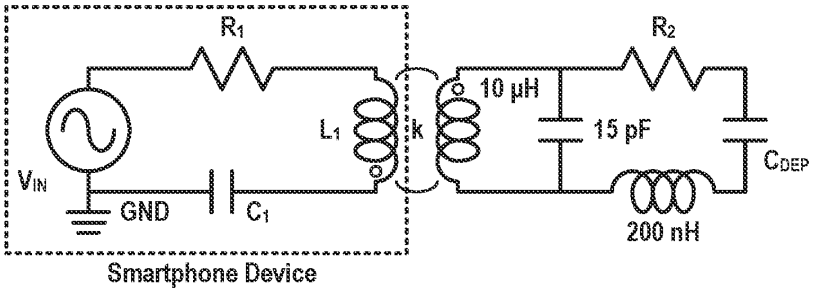

FIG. 15A

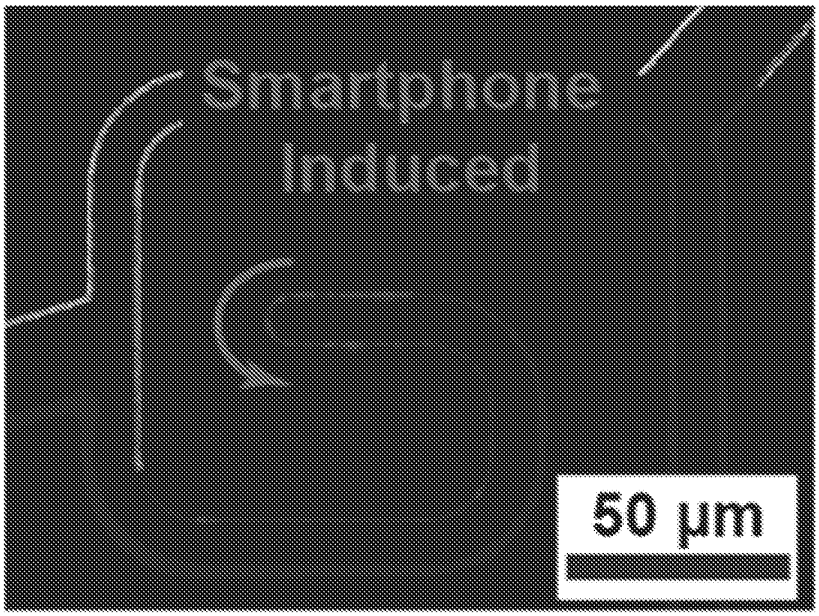

FIG. 15B

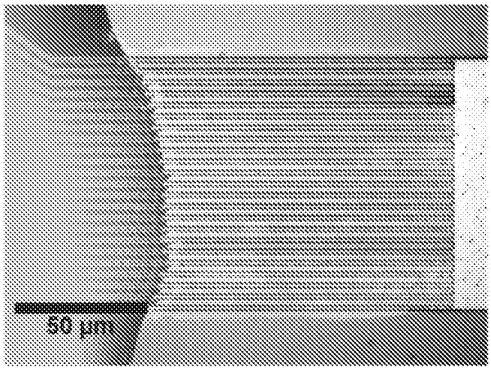

FIG. 16A

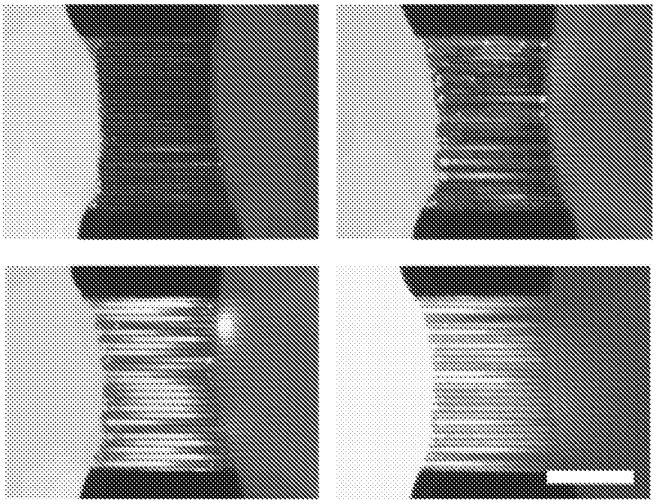

FIG. 16B

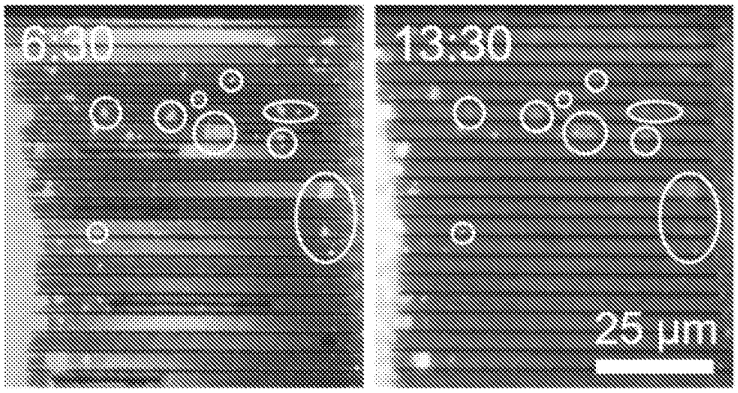

FIG. 16C

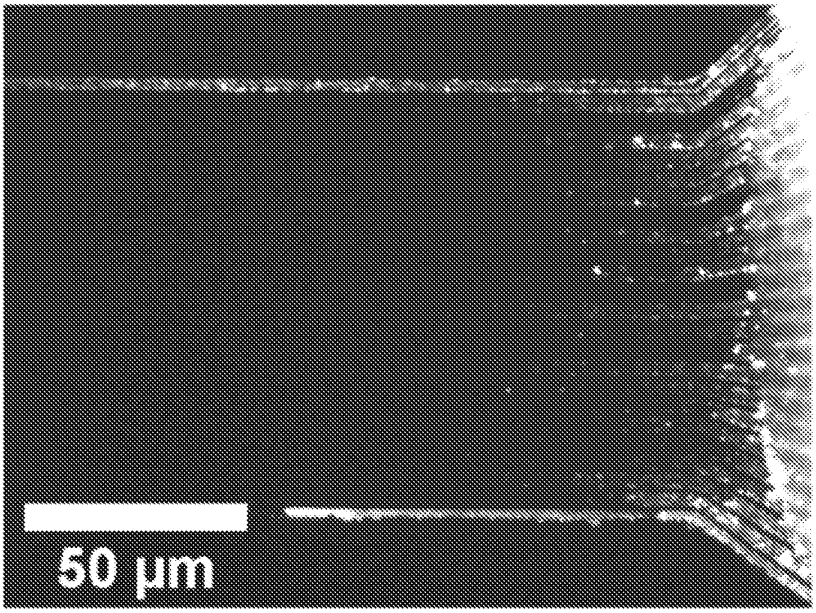

FIG. 17A

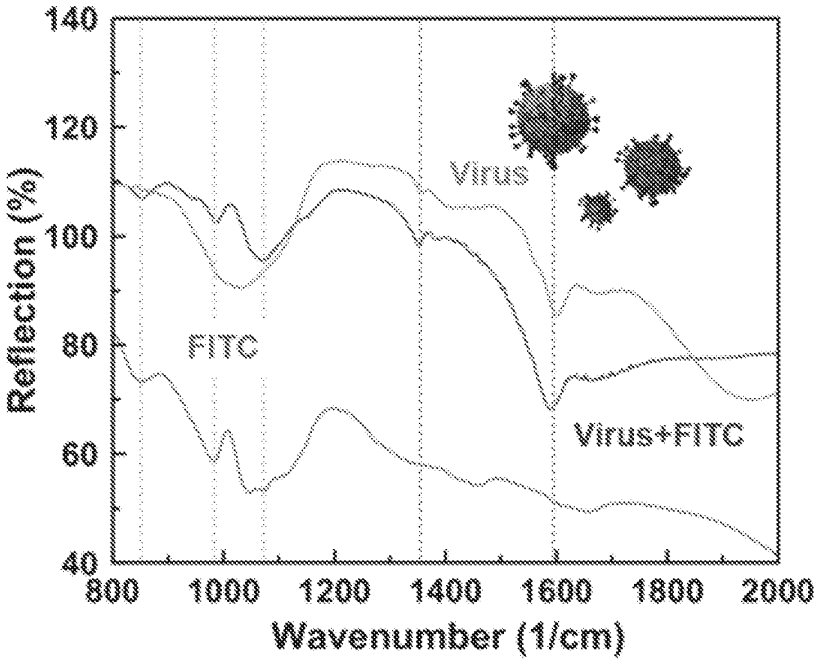

FIG. 17B

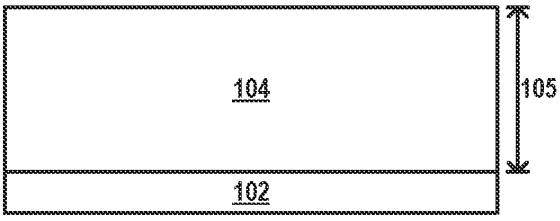

FIG. 18A

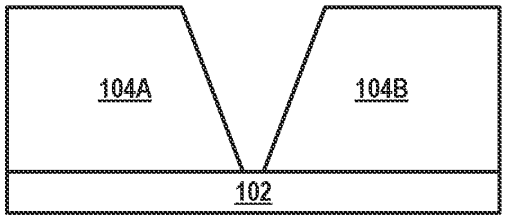

FIG. 18B

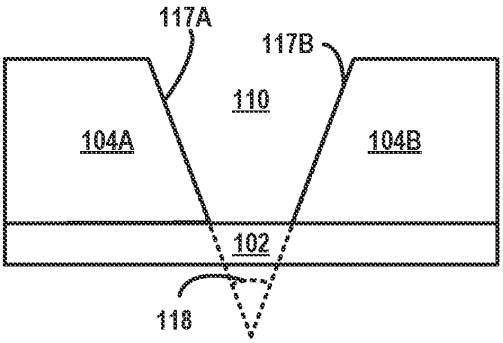

FIG. 18C

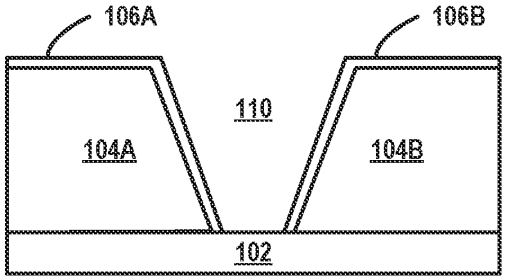

FIG. 18D

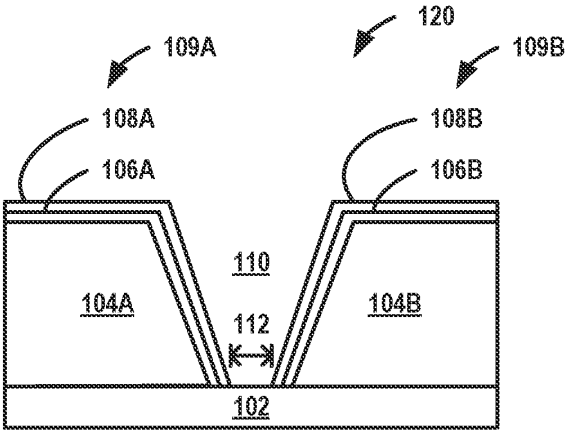

FIG. 18E

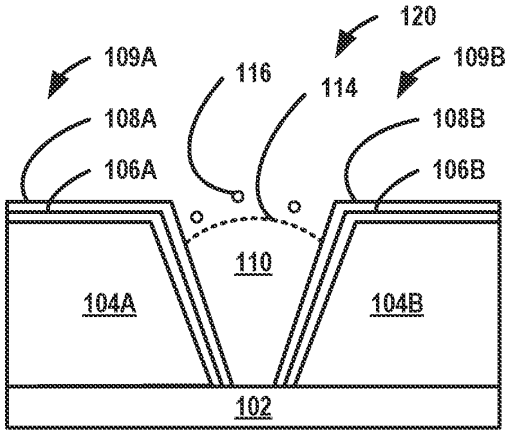

FIG. 18F

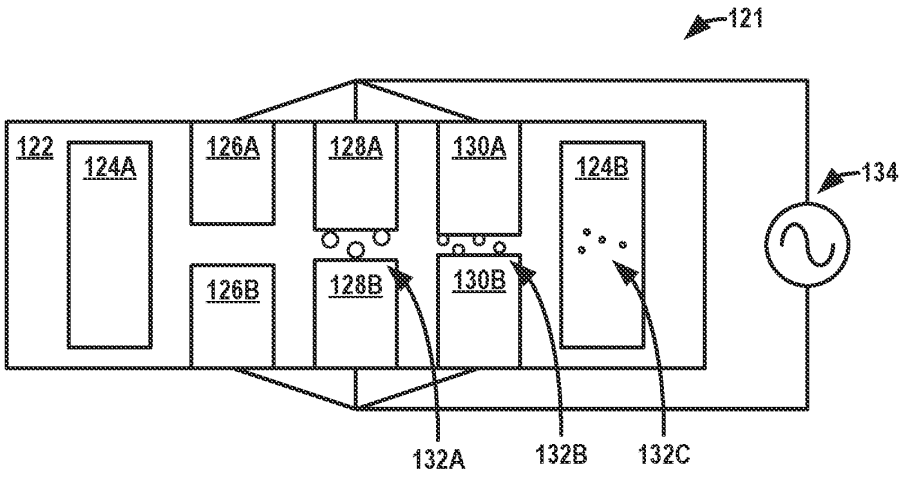
121
122
124A
126A
128A
130A
124B
134
126B
128B
130B
132A
132B
132C

FIG. 19

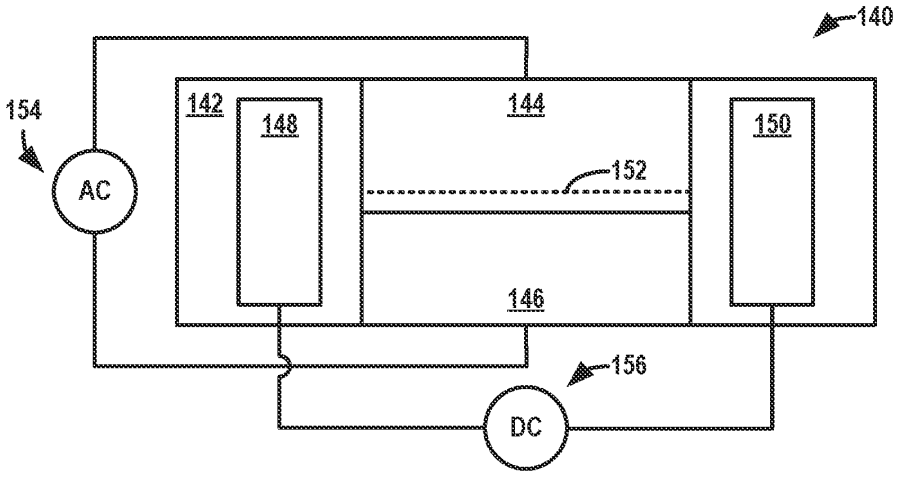
140
154
AC
142
148
144
150
152
146
156
DC

FIG. 20

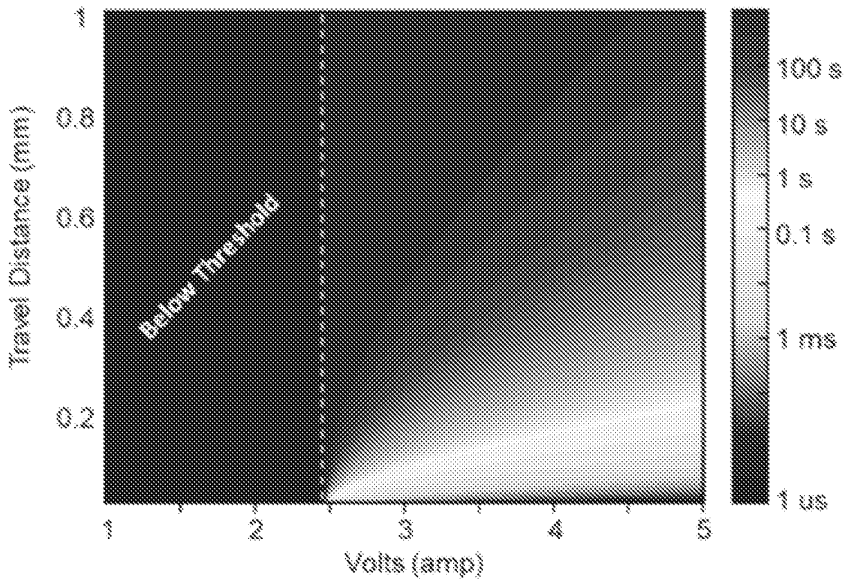
Travel Distance (mm)
1
0.8
0.6
0.4
0.2
Below Threshold
100 s
10 s
1 s
0.1 s
1 ms
1 us
1
2
3
4
5
Volts (amp)

FIG. 21

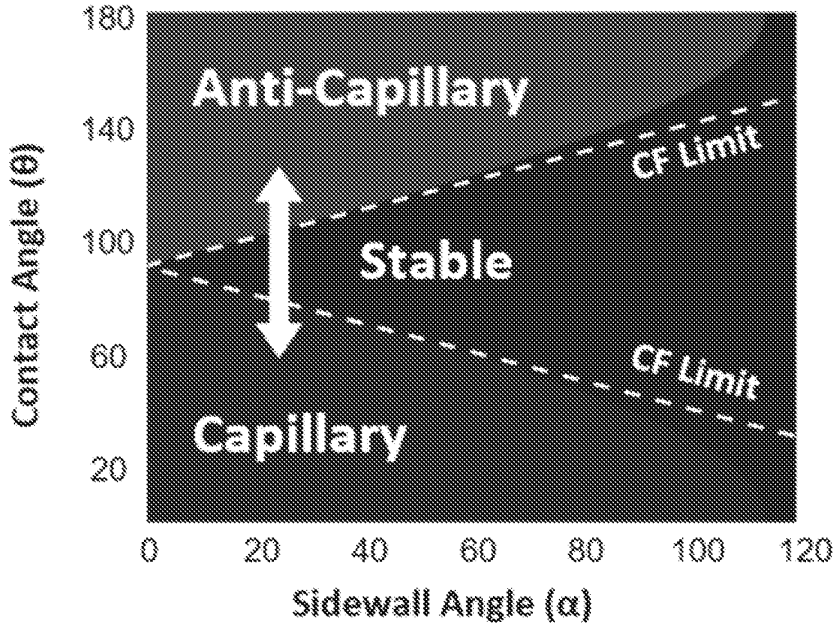
Contact Angle (θ)
180
140
100
60
20
Anti-Capillary
CF Limit
Stable
CF Limit
Capillary
0
20
40
60
80
100
120
Sidewall Angle (α)

FIG. 22